Design and Analysis of an X-Band Isolator Coupled to an Accelerating Manifold

Junaid Zafar
Faculty of Engineering, Government College University, Lahore, Pakistan
Email: chairperson.engineering@gcu.edu.pk

Tasneem Zafar
Department of Economics, Government College University, Lahore, Pakistan
Email: chairperson.economics@gcu.edu.pk

Andrew A. Gibson
School of Mechanical, Aerospace and Civil Engineering, The University of Manchester, UK
Email: Andrew.gibson@manchester.ac.uk

Haroon Zafar
Tissue Optics and Microcirculation Imaging Research Group, National University of Ireland, Galway, Ireland

***Abstract*—An X-band isolator was designed, simulated and developed for a colossal power X-ray beam emitter assembly. The developed isolator has been used to absorb reflection losses to protect the X-band magnetron source during experimental verification of emitter assembly characteristics. A finite element magnetostatic/microwave procedure is used to implement the phase control section of a 3-port isolator. This study decrees that the isolator has an operating bandwidth from 9.8-10.4GHz, manages peak power of 0.60MW, and an average power rating of 1.6KW. A minimum of 20-dB isolation with an insertion loss of less than 0.2dB over the operating frequency band was achieved. The microwave S-parameters computations fit well with the experimental data.**

***Index Terms*—insertion loss, isolation, phase control, magnetized waveguide**

I. Introduction

Magnetized ferrites based microwave isolators play a key role in high power source protection by absorbing reflections from manifold accelerating structures. They are commonly engaged in planar and waveguide-based structures to produce desired isolation and insertion phase control characteristics for microwave and mm- wave frequencies [1]. The development of these non-reciprocal devices at high power levels experience severe design challenges as non-linear spin wave losses dominate the microwave performance of magnetized ferrite structures [2]. Similarly at premium power thresholds other microwave losses and temperature dependence of material's magnetization are crucial to meet ever-increasing demands with enhanced power/frequency performance [1]-[3]. The thinner ferrite implants have the benefit of being easier to cool and helps in avoiding spin-wave manifold under certain magnetic bias conditions [3], [4]. The degeneration of microwave energy spectrum from spin-wave mode is realizable by calculating the spatial variation of the magnetic field and magnetization throughout the ferrite geometry and is described by the authors elsewhere [5], [6]. This paper presents a numerical procedure, which uses a magnetostatic solver to calculate the magnetic state of the ferrite prior to calculating the microwave characteristics. The computed magnetostatic result has been used as an input in the determination of microwave calculations. The operational frequency was used to construct a microwave permeability tensor and fed to the microwave solver to compute the insertion phase control for a given magnetized waveguide cross-section. This is an imperative development as low-field loss and nonlinear subsidiary resonance loss are both connected to bias field uniformity. The propagation wave numbers for forward and reverse energy movement were calculated and used further to work out the required phase isolation. The finite element (FE) calculations were demonstrated to agree well with the experimental data. The fabricated isolator is then coupled to a line shaped X- ray emitter and externally homogeneous magnetic field vicinity did the beam guidance. The detailed analysis for this uniform magnetic field vicinity has been described by the authors elsewhere [7], [8].

II. Dessign of a High Power Emitter Assembly

The developed system under consideration is presented in Fig. 1. It is comprised of an X-ray emitter coupled to a dielectric slab loaded manifold. An X-ray isolator has been designed and developed to protect the magnetron source from the microwave reflections originated by the

Manuscript received March 17, 2014; revised October 24, 2014.

doi: 10.12720/ijeee.3.5.385-389

waveguide accelerating structure [8]. The directly heated emitter has an emission surface length of 140 mm and the schematic cross sectional view of the developed emitter assembly is presented in Fig. 2. It delivers uniform current density throughout the entire line profile [8]. Circular cross-section line cathode was employed to generate electron beam with constant beam density along the line whereas the electromagnetic fields pattern help in eliminating any irregularities along the beam length regardless of the temperature [8].

The sequential steps involved in computer trace algorithm are illustrated in Fig. 3.

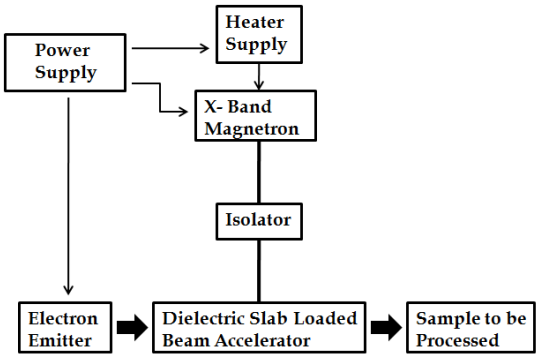

Figure 1. A schematic illustration of the set-up for experimental verification of microwave S-parameters.

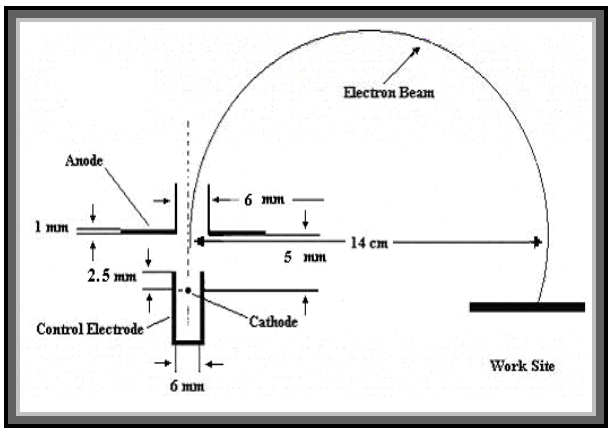

Figure 2. Schematic cross-section of the electron beam source.

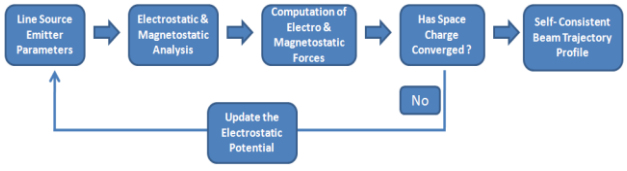

Figure 3. The computer trace of the electron beam trajectories.

III. Analysis of an X-Band Isolator

A key component in the accelerating manifold systems is the nonreciprocal isolator that allows the microwave engineers to control the microwave signal routing. A microwave isolator further helps in avoiding active stages from interfering and de-stabilizing one another, and absorbs reflections from high power waveguide based accelerators. A schematic illustration is presented in Fig. 4.

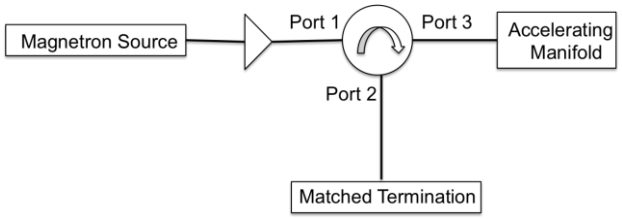

Figure 4. The role of an isolator in microwave signal routing.

The design and analysis of a high power microwave isolator require the knowledge concerning the electromagnetic and magnetostatic modes interaction [4]. To avoid non- linear spin wave losses, ferrite loaded isolators ensures frequency separation of the coupled mode from the spinwave manifold. The different mode regions for electromagnetic signal routing in an infinite gyromagnetic region are presented in Fig. 5.

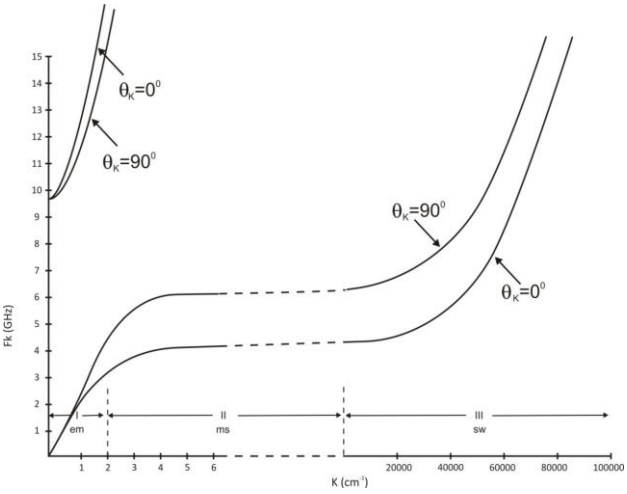

Figure 5. Different mode regions for wave propagation in an infinite gyromagnetic region. [Magnetization (M) = 140KA/m, Applied field (H) = 140KA/m, Exchange field (H_{ex}) = 39.7MA/m, ε_r = 15.9 and Lattice spacing (a) = 5×10^{-10}m

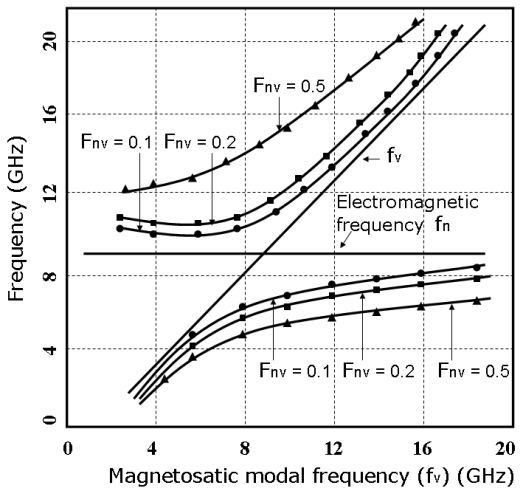

Figure 6. The segregation of uniform precession mode from spin-wave manifold for different coupling factors.

The solution of characteristic equation governing the interaction between an electromagnetic and magnetostatic mode for different values of coupling (F_{nv}) is presented in Fig. 6. This effect is associated with the decrease in the

magnetic linewidth together with an increase in non-linear threshold. One conventional method to avoid spin-wave instability is to increase the linewidth by doping but shortcoming associated with it is augmented small signal magnetic losses [4]. A second approach is to seek some means of avoiding the frequency relationship between the microwave signal and the spin- wave that is a prerequisite for the onset of spin-wave instability. This frequency condition involves the microwave frequency, ferrite magnetization, magnitude of magnetic field and shape and demagnetization factors of microwave geometry.

The design of a ferrite isolator is further complicated by the need for a bias field, nonlinear behavior and thermal dependencies. The requirement of the isolator design under consideration is to increase power/frequency performance and to reduce insertion loss. The magnetostatic and microwave calculations performed to realize a high power isolator are discussed in the subsequent sub- sections.

A. Magnetostatic Formulation

To construct the permeability tensor in terms of transverse field entries, the interior field and magnetisation inside ferrite vicinity has been determined using the magnetostatic analysis. The non- linear Poisson expression relating to longitudinal component of the magnetic vector potential (ϕ) was implemented [6], [9]. The demagnetising field expression was incorporated to account for surface variance of the magnetic fields and is given by (1).

$$\nabla_t \cdot (\mu_r^{-1} \nabla_t \phi) = -K \tag{1}$$

where K is the bias current density and μ_r^{-1} is described permeability tensor entries. The magnetization vector has been determined by using the expression in (2).

$$B = \mu_r H + M \tag{2}$$

B. Microwave Formulation

The numerical formulation based on finite element method has been used to calculate complex propagation wave number as an eigen vector [6]. The eigen values were found to be function of operational frequency, permittivity, and permeability tensor and magnetization vector. The presented formulation has used the expressions of orthogonal electric and magnetic fields [6], [9]. After applying specific boundary/sub-domain conditions and assimilating these equations on ferrite geometry's cross- section resulting in an expression given by (3).

$$\int_s \left[E_t^{test} . \omega \varepsilon_{tt} . E_t + H_t^{test} . \omega \mu_{tt} . H_t \right] ds$$

$$- \frac{1}{\omega \mu_{zz}} \int_s \left[\left[\nabla_t \times E_t^{test} \right] . \left[\nabla_t \times E_t + j\omega \mu_{zt} . H_t \right] - jH_t^{test} . \omega \mu_{tz} . \left[\nabla_t \times E_t + j\omega \mu_{zt} . H_t \right] \right] ds$$

$$- \frac{1}{\omega \varepsilon_{zz}} \int_s \left[\left[\nabla_t \times H_t^{test} \right] . \left[\nabla_t \times H_t - j\omega \varepsilon_{zt} . E_t \right] + jE_t^{test} . \omega \varepsilon_{tz} . \left[\nabla_t \times H_t - j\omega \varepsilon_{zt} . E_t \right] \right] ds$$

$$= \int_s - j\gamma z . \left[E_t^{test} \times H_t + E_t \times H_t^{test} \right] ds \tag{3}$$

The developed functional is implemented in COMSOL Multiphysics® and solution was achieved by performing a mesh analysis. The electric and magnetic fields profile inside differential elements were realized using weighted edge variables [6], [9]. The subsequent matrix expression inside every element module is illustrated in (4) and (5).

$$\begin{pmatrix} \omega\varepsilon A - 1/\omega\mu_{zz} B & j\omega\mu_{zt} C \\ -j\omega\mu_{tz} C^T & \omega[\mu_{tt} - (\mu_{zt}\mu_{tz})/\mu_{zz}]A - B/\omega\varepsilon \end{pmatrix} \tag{4}$$

$$\begin{pmatrix} a \\ b \end{pmatrix} = \beta \begin{pmatrix} 0 & D \\ D^T & 0 \end{pmatrix} \begin{pmatrix} a \\ b \end{pmatrix} \tag{5}$$

where a and b are weighted edge coefficients.

The sub-matrices can be easily computed using $\boldsymbol{N}$ as edge shape function using Eq. (6)-Eq. (9).

$$A_{ij} = \int [N^i \cdot N^j] dA \tag{6}$$

$$B_{ij} = \int [(\nabla_t \times N^i) \cdot (\nabla_t \times N^j)] dA \tag{7}$$

$$C_{ij} = \int [(\nabla_t \times N^i) \cdot N^j] dA \tag{8}$$

$$D_{ij} = \int [N^i \cdot N^j] dA \tag{9}$$

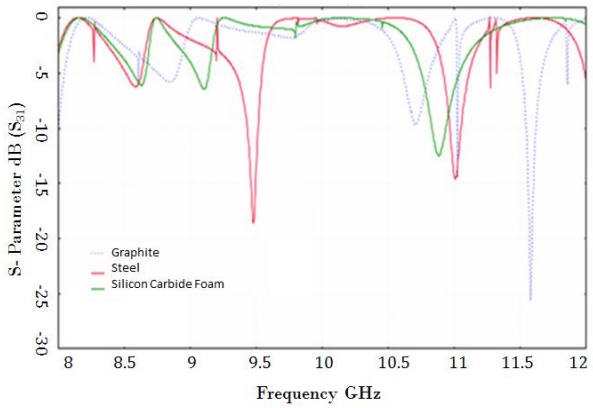

Figure 7. Insertion loss between port1 and port 3 using graphite, steel and silicon carbide termination at port 2.

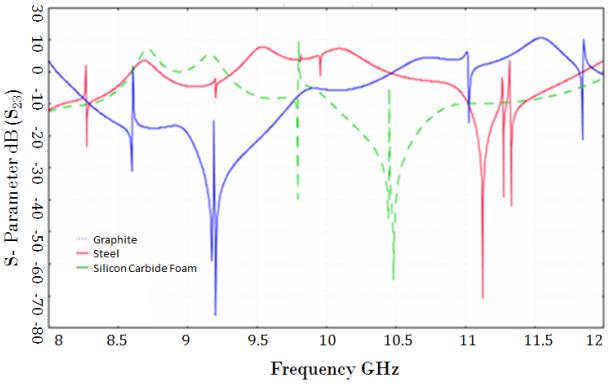

Figure 8. Isolation against bandwidth characteristics between port 2 and port 3.

IV. Results and Analysis

To analyze the microwave performance of the developed isolator, S-parameter analysis has been

performed. The transmission loss between port 1 and port 3 between the operational frequency range was found to be 0.2-dB as illustrated in Fig. 7.

The port 2 of the isolator has been perfectly matched and terminated using graphite, steel and silicon carbide termination. The isolation/bandwidth characteristics provided by the magnetized waveguide geometry is presented in Fig. 8.

The insertion loss against the frequency relationship has been experimentally verified and the results are presented in Fig. 9.

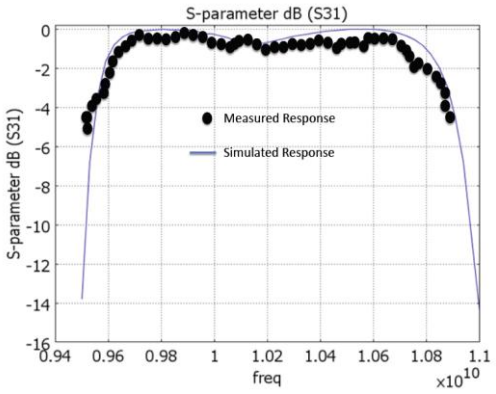

Figure 9. Simulated and measured results for insertion loss of the designed isolator.

The impact of permittivity and permeabilty of matched termination used to absorb microwave reflections from manifold structure are illustrated in Fig. 10 and Fig. 11 respectively.

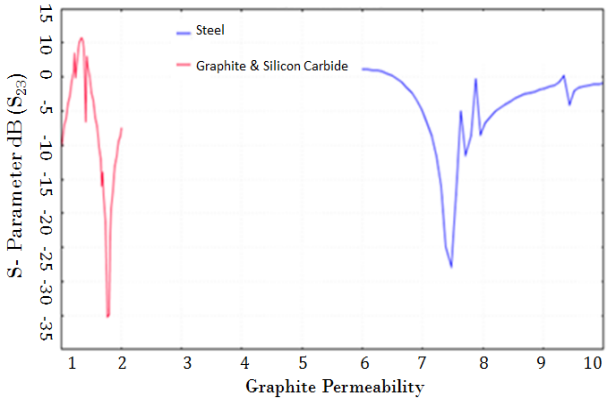

Figure 10. The effect of permeability on return loss between port 3 and port 2.

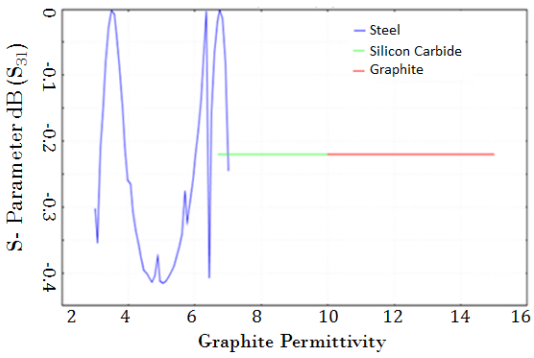

Figure 11. The effect of permittivity on return loss between port 3 and port 2.

The simulated insertion loss for a signal travelling from port 1 to port 3 is presented in Fig. 12.

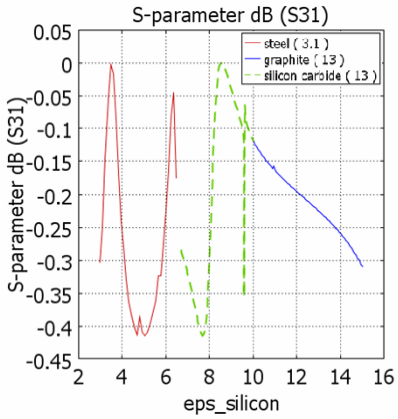

Figure 12. The insertion loss against permittivity between port 1 and port 3.

The measured return loss for reflected signal routing from port 1 to port 2 and from port 2 to port 1 is illustrated in Fig. 13.

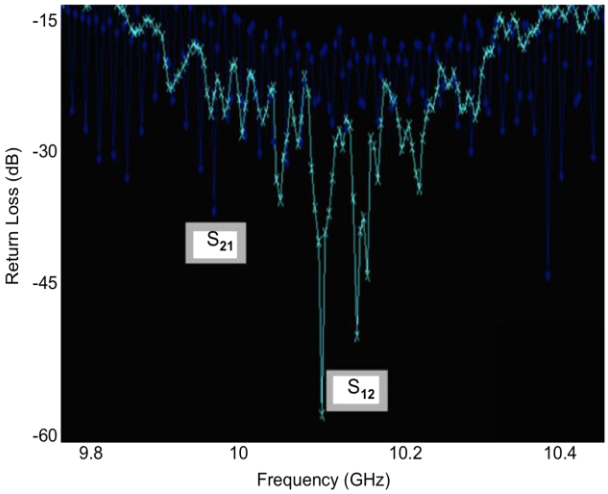

Figure 13. The measured return loss against frequency.

The isolation against the input power was measured and plotted in Fig. 14. A minimum of 18-dB isolation has been achieved over the desired band.

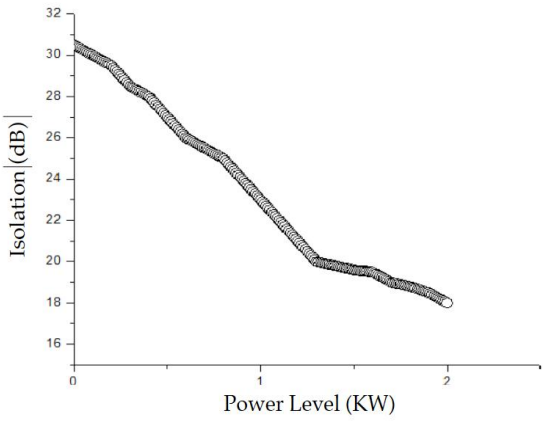

Figure 14. The experimental response of isolation characteristics against power.

The developed waveguide based ferrite isolator is illustrated Fig. 15.

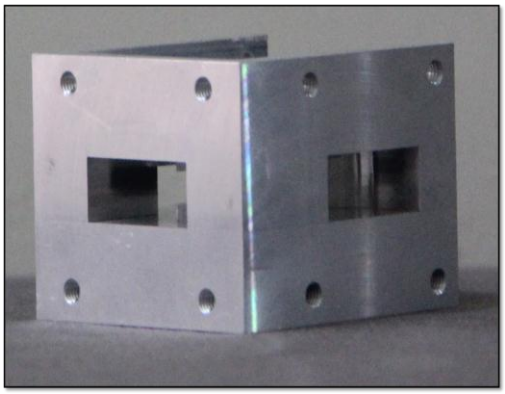

Figure 15. A snapshot of the developed X-band isolator.

V. Conclusion

An FEM based numerical functional has been used to design, simulate and develop an X-band isolator for a high power microwave signal routing. An operational bandwidth of 0.6GHz has been achieved with minimum isolation of 20-dB. The microwave performance in terms of S-parameters analysis has been evaluated, and found to be in well conformity with the simulated results.

References

[1] H. Razavipour, R. Safian, G. Askari, F. Fesharaki, and H. Sadeghi, "A new dual-band high power ferrite circulator," *Process in Electromagnetics Research C*, vol. 10, pp. 15-24, 2009.

[2] J. D Adam, L. E Davis, G. F Dionne, E. F Schloemann, and S. N Stitzer, "Ferrite devices and materials," *IEEE Transactions on Microwave Theory and Techniques*, vol. 50, pp. 721-737, 2002.

[3] J. Helszajn and P. N. Walker, "Operation of high peak power differential phase shift circulators at direct magnetic fields between subsidiary and main resonance," *IEEE Transactions on Microwave Theory and Techniques*, vol. 26, pp. 653-658, 1978.

[4] M. Weiner, "Electromagnetic effects in insulators," *J. Applied Physics*, vol. 43, pp. 1246-1255, 1972.

[5] B. M Dillon and A. A. P Gibson, "Analysis of partial-height ferrite-slab differential phase-shifter sections," *IEEE Transactions on Microwave Theory and Techniques*, vol. 48, no. 9, pp. 1577-1582, 2000.

[6] A. Abuelma'atti, J. Zafar, I. Khairuddin, A. A. P Gibson, A. Haigh, and I. Morgan, "Variable toroidal ferrite phase shifter," *IET Microwaves, Antennas and Propagation*, vol. 3, no. 2, pp. 1-8 2009.

[7] K. Masood, M. Iqbal, M. Zakaullah, J. Zafar, and A. A. P Gibson, "Influence of balancing parameters in achieving magnetic field uniformity in a large cylindrical volume," *Journal of Applied Physics*, vol. 104, pp. 014908, 2008.

[8] J. Zafar, H. Zafar, K. Masood, and A. A. P Gibson, "High emittance electron beam source coupled to slab loaded accelerating structure," *International Journal of Infrared and Millimetre Waves*, vol. 29, no. 12, pp. 1205-1214, 2008.

[9] J. Zafar, H. Zafar, and A. A. P Gibson, "Finite element analysis of a high power broadband circulator for air traffic surveillance radar system," in *Proc. International Conference on Radar Systems*, 2012, pp. 1-5.

